Redox Biology 38 (2021) 101830

Contents lists available at ScienceDirect

Redox Biology

journal homepage: www.elsevier.com/locate/redox

Hexameric procyanidins inhibit colorectal cancer cell growth through both redox and non-redox regulation of the epidermal growth factor signaling pathway

Elena Daveri [a,b,c], Ana M. Adamo [d], Eugenia Alfine [a,b], Wei Zhu [a,b], Patricia I. Oteiza [a,b,*]

[a] Departments of Nutrition University of California, Davis, 95616, Davis, CA, USA
[b] Departments of Environmental Toxicology, University of California, Davis, 95616, Davis, CA, USA
[c] Unit of Immunotherapy of Human Tumors, Fondazione IRCCS Istituto Nazionale dei Tumori, 20133, Milan, Italy
[d] Department of Biological Chemistry and IQUIFIB (UBA-CONICET), Facultad de Farmacia y Bioquímica, 1113, Universidad de Buenos Aires, Buenos Aires, Argentina

ARTICLE INFO

Keywords:
Proanthocyanidins
NADPH oxidase
Epidermal growth factor receptor
Colorectal cancer
Redox regulation

ABSTRACT

Dietary proanthocyanidins (PAC) consumption is associated with a decreased risk for colorectal cancer (CRC). Dysregulation of the epidermal growth factor (EGF) receptor (EGFR) signaling pathway is frequent in human cancers, including CRC. We previously showed that hexameric PAC (Hex) exert anti-proliferative and pro-apoptotic actions in human CRC cells. This work investigated if Hex could exert anti-CRC effects through its capacity to regulate the EGFR pathway. In proliferating Caco-2 cells, Hex acted attenuating EGF-induced EGFR dimerization and NADPH oxidase-dependent phosphorylation at Tyr 1068, decreasing EGFR location at lipid rafts, and inhibiting the downstream activation of pro-proliferative and anti-apoptotic pathways, i.e. Raf/MEK/ERK1/2 and PI3K/Akt. Hex also promoted EGFR internalization both in the absence and presence of EGF. While Hex decreased EGFR phosphorylation at Tyr 1068, it increased EGFR Tyr 1045 phosphorylation. The latter provides a docking site for the ubiquitin ligase c-Cbl and promotes EGFR degradation by lysosomes. Importantly, Hex acted synergistically with the EGFR-targeted chemotherapeutic drug Erlotinib, both in their capacity to decrease EGFR phosphorylation and inhibit cell growth. Thus, dietary PAC could exert anti-CRC actions by modulating, through both redox- and non-redox-regulated mechanisms, the EGFR pro-oncogenic signaling pathway. Additionally, Hex could also potentiate the actions of EGFR-targeted drugs.

1. Introduction

The epidermal growth factor (EGF) receptor (EGFR) has been extensively studied for its role in regulating a wide number of biological processes such as cell proliferation, survival, differentiation and migration [1,2]. In a pathological setting, dysregulation of the EGFR has been linked to the carcinogenic process of various epithelial human cancers, including colorectal cancer (CRC) [3]. Mechanisms identified in the oncogenic uncontrolled activation of the EGFR include gene amplification, protein overexpression, mutations and defective EGFR downregulation [4]. Such alterations in EGFR regulation leads to impaired control of cell apoptosis, enhanced proliferation, treatment refractoriness and poor clinical outcome [5].

CRC is a major public health concern, being the third most commonly diagnosed cancer in males and the second among females worldwide [6]. Signaling through the EGFR is frequently up-regulated in CRC, representing a promising therapeutic target for the inhibition of tumorigenesis in the intestinal tract [7]. EGFR-targeted therapies have been developed for the management of advanced CRC or tumors that are refractory to chemotherapy [8]. EGFR signaling can be targeted by either monoclonal antibodies, as cetuximab or panitumumab [9,10], which bind the extracellular domain of EGFR, or tyrosine kinase inhibitors, such as erlotinib or gefitinib [11,12], which interfere with the ATP-binding site of the EGFR catalytic domain. However, ongoing research has intensified efforts to develop adjuvant anti-cancer strategies in order to reduce the harmful side effects of chemotherapies and chemoresistance, as well as the risk of cancer development [13].

Diet has a major influence on cancer risk. CRC is particularly susceptible to dietary patterns given that intestinal cells are directly exposed to dietary components, and to the long multistep process

* Corresponding author. Departments of Nutrition and Environmental Toxicology, University of California, Davis, CA, USA.
E-mail address: poteiza@ucdavis.edu (P.I. Oteiza).

https://doi.org/10.1016/j.redox.2020.101830
Received 28 October 2020; Received in revised form 4 December 2020; Accepted 7 December 2020
Available online 10 December 2020

involved in CRC development, ranging from adenomatous lesions to the manifestation of malignant tumors. Furthermore, the intestinal epithelium is exposed to large amounts of dietary phytochemicals. Thus, the identification and promotion of long-term dietary consumption of phytochemicals could be a potential strategy in CRC prevention [14,15].

Among polyphenols, proanthocyanidins (PAC), oligomers of the flavan 3-ols (−)-epicatechin and (+)-catechin, are of raising interest for their ability to inhibit oncogenic signals [16–18] and have potential beneficial effects against CRC [19–21]. After dietary consumption, large PAC are not absorbed and reach the colon in significant amounts [22]. PAC oligomers of six subunits (Hex) inhibit in Caco-2 cells the deoxycholic acid acid-induced activation of oncogenic signals, i.e. ERK1/2/p38/AP-1 and Akt [23], in part by mitigating NADPH oxidase (NOX)-mediated transient $O_2^{\cdot-}/H_2O_2$ increases [24]. Hex also inhibits tumor necrosis factor alpha (TNF-α) induced activation of transcription factor NF-κB [25], which is involved in the crosstalk between inflammation and cancer [26]. Hex was shown to arrest the growth of several CRC cell lines and induce apoptosis via the mitochondrial pathway in Caco-2 cells [27]. Hex can also regulate cell signaling through selective Hex-cholesterol interactions at specialized cholesterol-enriched membrane rafts in Caco-2 cells [28]. Thus, the lipid raft-located and redox-sensitive EGFR emerges as a potential molecular target of Hex anti-CRC actions.

Overall, current evidence suggests that Hex could exert antitumorigenic effects at the gastrointestinal tract, inhibiting proproliferative pathways upon their interaction with the cell membrane. Knowing that a large number of membrane receptors, including the EGFR [29], are localized at lipid rafts where many transduction signals are initiated [30], and the widely described NOX-dependent redox regulation of EGFR activation [31], we investigated if Hex could inhibit CRC cell growth through both, the redox-dependent and independent modulation of the EGFR signaling pathway. We evaluated the capacity of Hex to: (i) inhibit the activation and dimerization of the EGFR upon EGF-stimulation, (ii) inhibit EGFR activation by decreasing the production of reactive oxygen species (ROS) through NOX modulation, iii) prevent the activation of the main downstream signaling pathways, i.e. Raf/MEK/ERK1/2 and PI3K/Akt, (iv) modulate the internalization of the receptor, (v) promote EGFR degradation and (iv) cooperate with a currently used chemotherapeutic drug (Erlotininb) which inhibits EGFR activity. The interactions of Hex with the cell membrane and the inhibition of EGF-mediated transient increased production of reactive oxygen species (ROS), could explain the capacity of Hex to modulate EGFR activity and downstream events.

2. Materials and methods

2.1. Materials

The human colorectal adenocarcinoma cell line Caco-2 was obtained from the American Type Culture Collection (Manassas, VA, USA). Cell culture media and reagents were from Gibco (Gaithersburg, MD, USA). EGF, human recombinant, was obtained from Corning Inc. (Corning, NY, USA). Primary antibodies against EGFR (D38B1) (#4267), p (Tyr 1068)-EGFR (#3777), p (Tyr 1045)-EGFR (#2237), c-Raf (#9422), p (Ser 338)-c-Raf (#9427), MEK (#9122), p (Ser 217/221)-MEK (#9154), ERK 1/2 (#9102), p (Thr 202/Tyr 204)-ERK1/2 (#9101), p (Tyr 458/Tyr 199)-PI3K (#4228), Akt (#9272), p (Thr 308)-Akt (#9275), c-Cbl (C49H8) (#2179), ubiquitin (P4D1) (#3936), secondary antibodies anti-rabbit HRP-conjugated (#7074) or biotinylated (#14708) and biotinylated ladder (#7727) were from Cell Signaling Technology, Inc. (Danvers, MA, USA). Primary antibodies against α-tubulin (sc-9104), flotillin-1 (H-104) (sc-25506), LAMP-1 (H-228) (#sc-5570), agarose A/G beads (sc-2003) and secondary anti-mouse IgG1 HRP-conjugated (#2969) were from Santa Cruz Biotechnology (Santa Cruz, CA, USA). Cy 2- conjugated donkey anti-mouse IgG (#715-225-150) and Cy3-conjugated goat anti rabbit IgG (#111-165-003) were from Jackson ImmunoResearch Laboratories, Inc. (West Grove, PA, USA). The protease and phosphatase inhibitor cocktail was from Roche Applied Science (Mannheim, Germany). Colored standards and all the other reagents for Western blot were from Bio-Rad Laboratories Inc. (Hercules, CA, USA). Mouse monoclonal antibody against EGFR Ab-3 (#MS-311-P0), IP-Lysis Buffer (#87787), Pierce ECL Western Blotting Substrate and Hoechst 33,342 were from Thermo Fisher Scientific (Waltham, MA, USA). 3,3′,5,5′-dihydroethidium (DHE) was from EMD Millipore (Hayward, CA). Apocynin, diphenyleneiodonium (DPI), *N*-ethylmaleimide, OptiPrep, sulphorhodamine B, suberic acid bis(3-sulfo-*N*-hydroxysuccinimide ester) (BS3), tetramethylbenzidine (TMB) and VAS-2870 were from Sigma-Aldrich (St. Louis, MO, USA). CellTiter-Glo® Luminescent Cell Viability assay was from Promega (Madison, WI). Erlotinib (E−4007) was from LC Laboratories (Woburn, MA, USA). 5-(and-6)-carboxy-2′,7′-dichlorodihydrofluorescein diacetate (DHDCF) and Amplex Red Hydrogen Peroxide/Peroxidase Assay Kit were from Invitrogen/Life Technologies (Grand Island, NY). Hexameric procyanidins (Hex) source and characterization was previously described [23].

2.2. Cell cultures and incubations

Caco-2 cells were cultured at 37 °C under a 5% (v/v) CO_2 in Minimum Essential Medium (MEM) supplemented with 10% (v/v) FBS and antibiotics (50 U/ml penicillin, and 50 μg/ml streptomycin), 1 mM sodium pyruvate and 1% (v/v) of non-essential amino acids. The medium was replaced every 3 days and cells were used for experiments when they had reached up to a 60% confluence. Cells were starved in serum-free media for 24 h and then cells were incubated in the absence/presence of 2.5, 5, 10 μM Hex for 30 min at 37 °C, without or with subsequent stimulation with 10 ng/ml EGF at 37 °C for 10 min.

2.3. Evaluation of cytotoxicity

To evaluate the cytotoxic activity of Hex and Erlotimib, cell viability was assessed using the CellTitle-Glo® Luminiscent Cell Viability assay. To assure an exponential growth for the whole duration of the experiment, Caco-2 cells were seeded in 96-well plates at a density of 5×10^3 cells/well. 24 h later, cells were treated with 0.5–30 μM Hex or Erlotinib for 72 h. For each compound, results are expressed as relative percent luminescence compared to controls. Hex and Erlotinib concentrations that yielded 50% cell inhibition (IC_{50}) were calculated by non-linear least-squares curve-fitting (Prism GraphPad Software Inc., San Diego, CA).

2.4. Drug combination studies

For the combination studies, the two compounds were added at a non-constant ratio [32]. Caco-2 cells treated with increasing concentrations of Hex (0.5–30 μM) were simultaneously exposed to a fixed Erlotinib concentration (IC_{25}). The cytotoxicity of the combination was compared with the cytotoxicity of each compound alone using the combination index (CI) from the Chou and Talalay method [33], where $CI < 1$, $CI = 1$, $CI > 1$ denotes synergism, additive interaction and antagonism, respectively. Data analysis were carried out using the CompuSyn software (ComboSyn Inc, Paramus, NJ).

2.5. Protein extraction and western blot analysis

For the preparation of total cell extracts, after the corresponding treatments, cells were rinsed with PBS, scraped and centrifuged. To prepare total cell extracts, the pellet was suspended in 40 μL of IP-Lysis Buffer containing protease and phosphatase inhibitors. Samples were incubated at 4 °C for 30 min, and centrifuged at 15,000×*g* for 30 min. Protein concentration in the supernantants was measured using the Bradford assay [34]. Aliquots of total cell fractions containing 20–30 μg protein were separated by reducing 4–20% (w/v) polyacrylamide gel

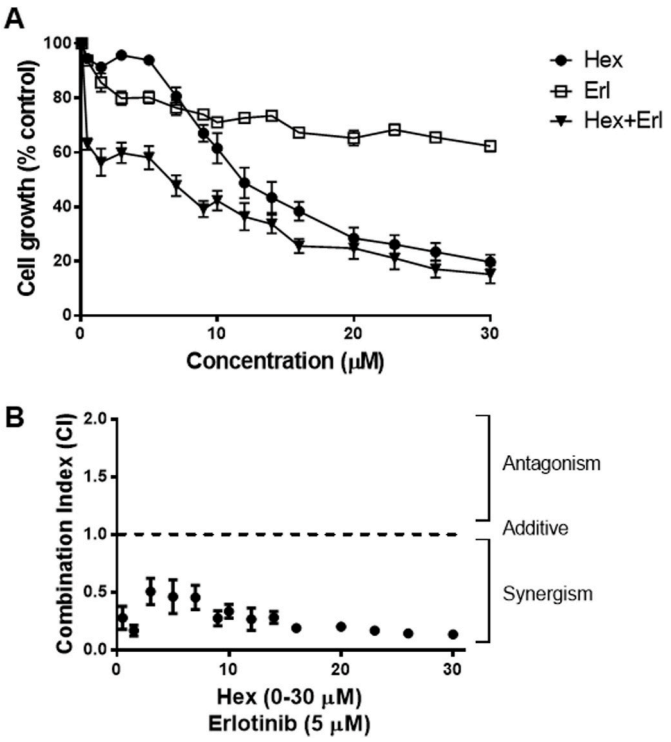

Fig. 1. Cytotoxicity and pharmacological interaction of Hex and Erlotinib in Caco-2 cells. (A) Representative curves of growth inhibitory effects of Hex, Erlotinib and Hex-Erlotinib in non-fixed combination after simultaneous incubation for 72 h. (B) CI values for Hex-Erlotinib simultaneous combination, where CI < 1, C = 1 and CI > 1 represents synergism, additive and antagonistic interactions, respectively. Results are shown as mean ± SEM and are the average of at least three independent experiments, each run in triplicates.

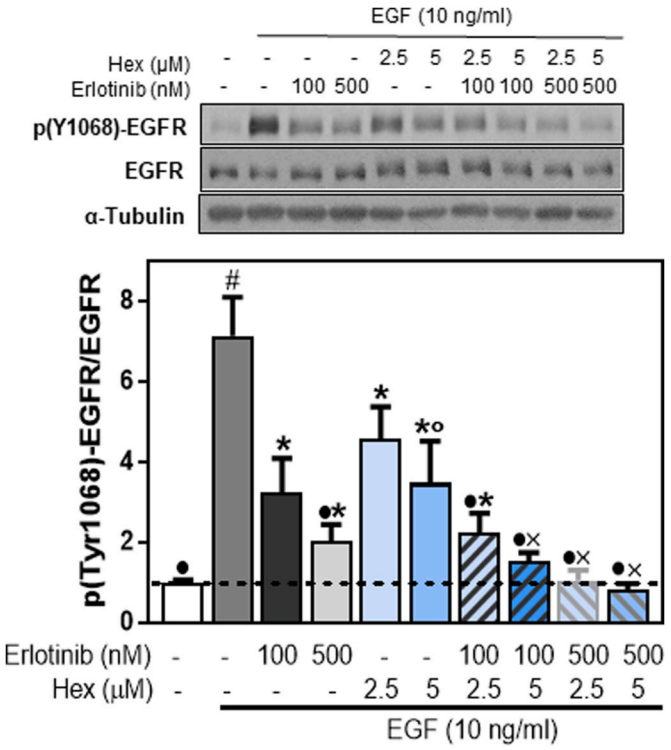

Fig. 2. Effects of Erlotinib, Hex and their combination on EGFR phosphorylation (Tyr1068).
Levels of p
(Tyr1068)-EGFR were measured by Western blot. Caco-2 cells were added with 100 and 500 nM Erlotinib, 2.5 and 5 μM Hex, and their simultaneous combination. After 30 min incubation at 37 °C, cells were incubated for further 10 min in the absence or the presence of EGF (10 ng/ml). After Western blots, bands were quantified and values for p (Tyr1068)-EGFR referred to total EGFR content. Results were referred to control values (1, dashed line). Results are shown as mean ± SEM and are the average of at least five independent experiments. Values having different superscripts are significantly different ($p < 0.05$, One way ANOVA).

electrophoresis and electroblotted to PVDF membranes. Colored and biotinylated molecular weight standards were ran simultaneously. Membranes were blotted for 1 h in 5% (w/v) non-fat milk, incubated overnight in the presence of the corresponding antibodies (1:500–1:1.000 v/v) in 5% (w/v) BSA in TBS buffer (50 mM Tris, 150 mM NaCl, pH 7.6), containing 0.1% (v/v) Tween-20. After incubation for 90 min at room temperature in the presence of the secondary antibody (HRP-conjugated) (1:10.000 v/v), the conjugates were visualized by chemiluminescence using an ECL reagent, and detected in a Phosphoimager 840 (Amersham Pharmacia Biotech. Inc., Piscataway, NJ).

2.6. Cell oxidant levels

Cell oxidant levels were estimated using the probes DCFDA, DHE and Amplex red. DCFDA and DHE enter cells, and when oxidized are converted into fluorescent compounds. Caco-2 cells were plated in 96-well plates (5×10^4 cells/well), grown up to 60–70% confluency and then starved for 24 h prior to the experiments. Cells were then pretreated for 30 min with or without 5 μM Hex, 1 μM apocynin, 1 μM VAS-2870 or 1 μM DPI, and subsequently incubated for 0–2 h in the absence or the presence of EGF (10 ng/ml). At the different time points, cells were added with 20 μM DCFDA or 25 μM DHE, and after 30 min incubation, the medium was removed and cells rinsed with PBS. Fluorescence was measured, for oxidized DCFDA at λexc: 495 nm; λem: 520 nm, and for oxidized DHE at λexc: 518 nm; λem: 605 nm H_2O_2 released to the medium was measured at the corresponding time points with the Amplex® Red Hydrogen Peroxide/Peroxidase Assay Kit following the manufacturer's protocol. To normalize for the number of cells, fluorescence was referred to protein content measured by reaction with sulphorhodamine B [35]. Fluorescence and absorbance were measured using a Biotek Synergy H1 plate reader (BioTek Instruments, Winooski, VT).

2.7. Receptor dimerization

Receptor dimerization was measured according to the method of Turk and Chapkin [36]. Briefly, cells treated as described above, were washed with PBS, and plates were subsequently added with 3 mM BS3 in Ca^{+2}/Mg^{+2}-free PBS and incubated on ice for 20 min. BS3 is a bifunctional cross-linking compound that, under the current experimental conditions, will form amides by reaction with membrane protein amino groups. This reaction was quenched by adding 250 mM glycine in PBS and incubating for 5 min on ice. Cells were washed with PBS and samples processed as usual to obtain total homogenates. Protein concentration was measured and the presence of EGFR dimers was assessed by Western Blot analysis.

2.8. Lipid rafts isolation

Lipid rafts were isolated using a non-detergent method basically as described by Macdonald and Pike [37]. All procedures were carried out at 4 °C. Caco-2 cells grown in 150 mm^2 dishes were serum-starved for 24 h and treated with or without 5 and 10 μM Hex, and in the absence or the presence of 10 ng/ml EGF for the indicated periods of time. Cells were collected in Base Buffer (20 mM Tris-HCl pH 7.8, 250 mM sucrose, 1 mM $CaCl_2$, 2.5 mM $MgCl_2$) containing protease and phosphatase inhibitors. Cells were passed 20 times through a 22 g x 3″ needle and the cell homogenates were centrifuged for 10 min at 1.000×*g*. After collecting the supernatant, the pellet was submitted to another cycle of

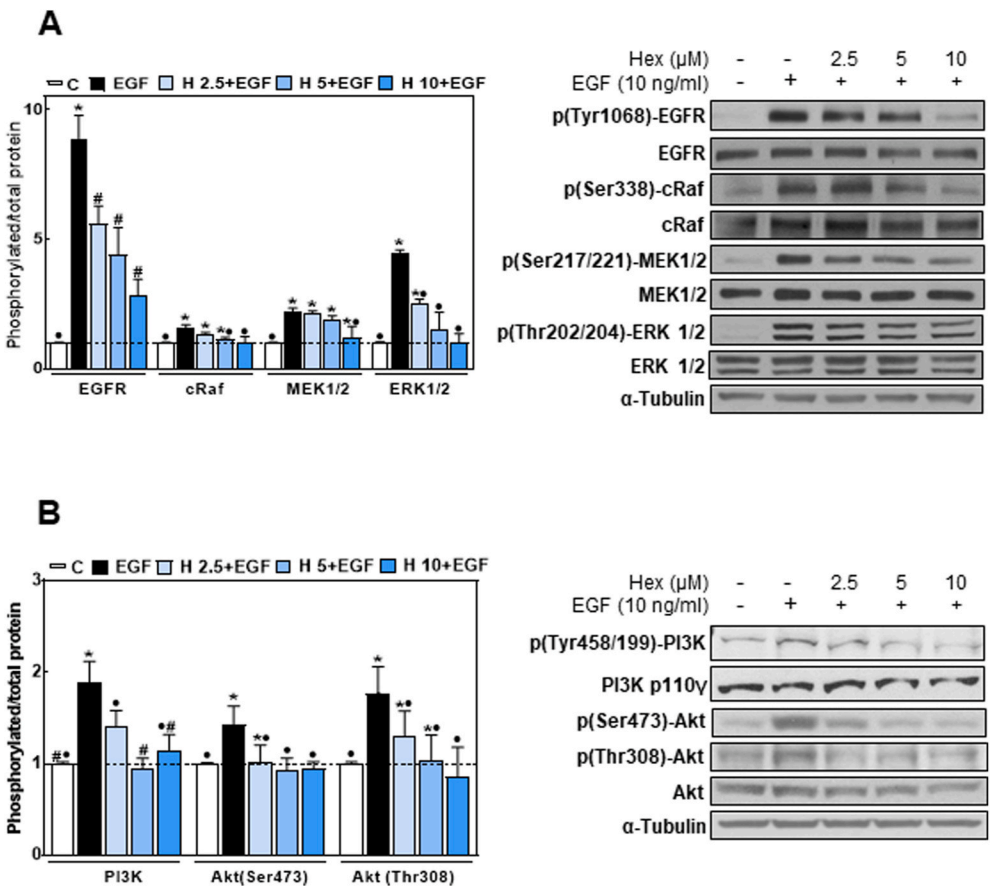

Fig. 3. Hex inhibits signal activation downstream the EGFR. Caco-2 cells were incubated without or with 2.5, 5 and 10 μM Hex for 30 min at 37 °C and subsequently incubated in the absence/presence of EGF (10 ng/ml) for 10 min at 37 °C. Western blot images show (A) p (Tyr1068)-EGFR, EGFR, p (Ser338)-cRaf, cRaf, p (Ser217/221)-MEK1/2, MEK1/2, p (Thr202/204)-ERK1/2, ERK1/2 and α-tubulin, and (B) p (Tyr458/199)-PI3K, PI3K p110γ, p (Ser473)-Akt, p (Thr308)-Akt, Akt and α-tubulin in total cell extracts. After Western blots, bands were quantified and values for the phosphorylated proteins were referred to the total content of the corresponding protein. Results were referred to control values (1, dashed line). Results are shown as mean ± SEM and are the average of at least five independent experiments. Values having different superscripts are significantly different ($p < 0.05$, One way ANOVA).

passage through the needle and centrifugation. Supernatants, resulting from the first and the second centrifugation, were combined and added with Optiprep to a final 45% (v/v) OptiPrep concentration. Two layers of 5% and 35% OptiPrep in Base Buffer, respectively, were poured on top of the 45% lysate solution. Lipid rafts were isolated by centrifugation in a swinging bucket rotor for 150 min at 53.000×*g* in a Sorvall RCM120 GX centrifuge (Thermo Scientific, New York, NY, USA). 200 μL fractions were taken from the top to the bottom of the tube and the distribution of EGFR and flotillin-1 was evaluated by Western blot.

2.9. Receptor internalization analysis

The ability of Hex to induce EGFR internalization was determined by a cell-ELISA assay. Caco-2 cells were cultured in 96-well plates and, after starvation for 24 h, they were incubated with or without 2.5–10 μM Hex and/or 10 ng/ml EGF. Plates were subsequently incubated on ice for 30 min to allow the binding of the ligand (EGF) to the receptor. Subsequently, cells were incubated for 15 min at 37 °C to allow EGFR internalization. After washing, cells were fixed with 2% (w/v) paraformaldehyde for 20 min at room temperature and blocked with 1% (w/v) BSA in PBS for 1 h at room temperature. The *anti*-EGFR antibody (1:200 v/v in 1% (w/v) BSA) was added and cells incubated for 2 h at room temperature. Plates were washed and incubated with a HRP-conjugated secondary antibody (1:10.000 v/v) in 1% (v/v) BSA for 90 min at room temperature. Cells were rinsed with PBS and incubated with 100 μL of 3,3′,5,5′-tetramethylbenzidine (TMB) substrate (ready-to-use solution) at room temperature in the dark. After 10 min incubation, the enzymatic reaction was stopped by addition of 100 μl of 1 M H_2SO_4. The absorbance at 450 nm was measured with a microplate reader (Wallac 1420 VICTOR2TM PerkinElmer Life Science, Waltman, USA).

2.10. Immunocytochemistry

The intracellular localization of the receptor was evaluated by immunofluorescence staining. Caco-2 cells were cultured on polylysine-coated coverslips. Caco-2 cells were starved for 24 h, then treated in the presence/absence of 10 μM Hex for 30 min at 37 °C, and stimulated with 10 ng/ml EGF for 10 and 20 min at 37 °C. After washing, cells were fixed with 4% (w/v) paraformaldehyde for 20 min at 4 °C. Fixed cells were permeabilized and blocked by incubation with 0.1% (v/v) Triton X-100 and 0.1% (v/v) donkey serum for 30 min at room temperature. Coverslips were incubated overnight at 4 °C with primary antibodies against EGFR Ab-3 (1:100 v/v) and LAMP (1:500 v/v) in 0.1% (v/v) donkey serum. Coverslips were rinsed in PBS and incubated for 2 h at room temperature with a Cy2-conjugated donkey anti-mouse IgG (1:500 v/v) and Cy3-conjugated goat anti rabbit IgG (1:500 v/v) antibodies for 2 h at room temperature. Cell nuclei were stained with Hoechst 33,342 and preparations were visualized by laser confocal microscopy using an Olympus FV 300 microscope.

2.11. Co-immunoprecipitation

To assess the ubiquitination status of the EGFR, Caco-2 cells were plated on 100 mm^2 dishes, serum starved for 24 h and incubated with or without 5 and 10 μM Hex in the presence of 10 ng/ml EGF at 37 °C for the indicated periods of time. Cells were subsequently washed with ice-cold Ca^{2+}, Mg^{2+} -free PBS and lysed in a modified RIPA buffer containing 10 mM *N*-ethylmaleimide, 1 mM Na_3VO_4, and protease/phosphatase inhibitor cocktails. The EGFR was immunoprecipitated with a monoclonal mouse *anti*-EGFR antibody on agarose A/G beads for 1 h at 4 °C. After centrifugation, beads were washed three time with the complete lysis buffer, resuspended in Laemmli sample buffer, and heated at 95 °C for 5 min. The lysates and immunoprecipitates were

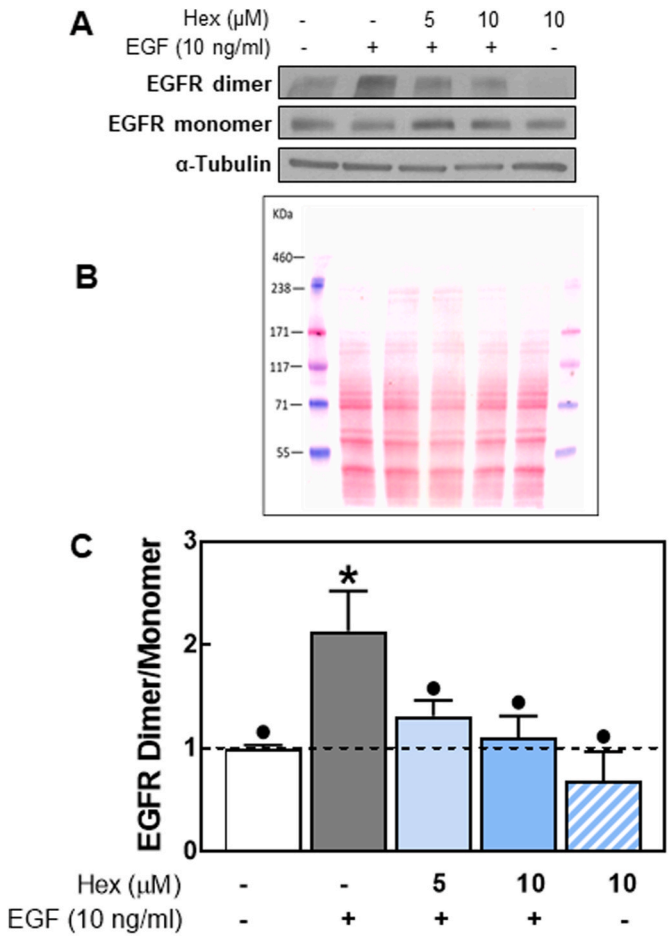

Fig. 4. Effects of Hex on EGFR dimerization.
Serum starved Caco-2 cells were treated with/without Hex (5 and/or 10 μM) and in the absence or presence of EGF (10 ng/ml), for 1 h at 4 °C. Cell membrane receptors were cross-linked with 3 mM BS3 as described in methods. EGFR monomers and dimers were assessed by Western blot. Upon stimulation with EGF, EGFR dimers were identified as a band twice the molecular weight (340 kDa) of EGFR monomers (170 kDa). (A) Representative Western blot images, (B) protein loading was assessed by Ponceau staining and (C) bands were quantified and the ratio dimers/monomers calculated and referred to control (cells incubated in the absence of additions) values (1, dashed line). Results are shown as mean ± SEM and are the average of at least three independent experiments. Values having different superscripts are significantly different ($p < 0.05$, One way ANOVA).

resolved by 6% (w/v) SDS-PAGE followed by transfer to PVDF membranes and blotting with antibodies against EGFR, p (Tyr 1068)-EGFR, c-Cbl and ubiquitin.

2.12. Statistical analysis

Data were analyzed by one-way analysis of variance (ANOVA) using Statview 5.0 (SAS Institute Inc., Cary, NC, USA). Fisher's Least Significance Difference test was used to examine differences between group means. A p value < 0.05 was considered statistically significant. Results are shown as mean ± SEM of at least three independent experiments.

3. Results

3.1. Evaluation of the antiproliferative activity of Hex and Erlotinib and combination analysis

We initially investigated the potential interactions between Hex and the EGFR-targeting drug Erlotinib in decreasing Caco-2 cell viability (**Fig. 1**). Cells were incubated in the absence or presence of 0.5–30 μM Hex or Erlotinib for 72 h. Hex inhibited cell growth in a dose-dependent manner, with an IC_{50} value of 12 μM (**Fig. 1A**). The sensitivity of Caco-2 cells to Erlotinib was not dose-dependent and cell growth inhibition did not reach 50% at the highest concentration tested (30 μM). Next, the growth-inhibitory effect of Hex in combination with Erlotinib was evaluated. Because drugs were not equipotent, the combination study was performed using non-fixed ratios, as described in methods, at the IC_{50} concentration for Hex and IC_{25} for Erlotinib (5 μM) (Fig. 1A and B). Fig. 1B shows the average of the combination index (CI) values for the Hex-Erlotinib treatment. These results indicate that the combined effect of Hex and Erlotinib on cell cytotoxicity is synergistic ($CI < 1$).

3.2. Combined effects of Hex and Erlotinib at decreasing EGFR phosphorylation

Erlotinib acts inhibiting the EGFR tyrosine kinase activity. We next investigated if Hex and Erlotinib synergism also occurs at the level of EGFR phosphorylation at Tyr1068. Cells were incubated with or without 2.5 and 5 μM Hex, 100 and 500 nM Erlotinib or their combination (Fig. 2) followed by incubation in the presence or the absence of EGF for subsequent 10 min. EGFR Tyr1068 phosphorylation was evaluated by Western Blot. A partial inhibition in EGFR Tyr1068 was observed at 100 and 500 nM Erlotinib (55 and 72%, respectively) and at 2.5 and 5 μM Hex (35 and 50%, respectively). However, simultaneous treatment with Hex and Erlotinib at the concentration that caused a 50% decrease of EGFR Tyr1068 phosphorylation (5 μM and 100 nM, respectively), fully inhibited EGF-induced EGFR phosphorylation (Fig. 2).

3.3. Hex reduced EGF-induced activating phosphorylation of the EGFR and downstream target proteins

Given the importance of the EGFR in human cancer by influencing cell proliferation, survival and metastatic potential [38], we next investigated the effects of Hex on the receptor tyrosine kinase activity and downstream proliferative signaling pathways. EGF caused a 4.5-fold increase in EGFR phosphorylation at the tyrosine residue 1068 (Fig. 3A). Hex decreased this phosphorylation in a concentration (2.5–10 μM)-dependent manner (Fig. 3A). We next investigated the effects of Hex on the downstream activation of both Ras/MEK/ERK1/2 and PI3K/Akt cascades. As shown in Fig. 3A and **B**, Hex decreased in a dose-dependent manner the phosphorylation of c-Raf (Ser 338), MEK1/2 (Ser 217/221), ERK 1/2 (Thr 202/Tyr 204), PI3K (Tyr 458/199) and Akt (Thr 308 and Ser 473). At 10 μM concentration, Hex almost fully inhibited EGF-induced activation of both pathways.

3.4. Hex reduced EGFR dimer formation

We next evaluated if Hex could inhibit the dimerization of the receptor occurring upon EGF binding. Caco-2 cells were pretreated with or without Hex (5 and 10 μM) and subsequently incubated for 1 h in the presence or the absence of EGF (10 ng/ml). Cells were subsequently incubated with the membrane-impermeable protein cross-linker BS3, and EGFR dimerization was evaluated by Western blot. EGF caused a 2.1-fold increase in EGFR dimer formation compared to basal levels (Fig. 4). Incubation with 5 or 10 μM Hex decreased EGF-induced EGFR dimerization.

3.5. Hex mitigates the NOX-dependent activation of the EGFR

The activation of the EGFR is associated with NOX activation leading to transient ROS increases which enhance/extend the EGFR signaling pathway [31,39]. Thus, we next investigated if Hex could in part inhibit EGFR activation by decreasing EGF-mediated ROS increase. We studied the capacity of Hex and three NOX inhibitors to mitigate EGF-mediated

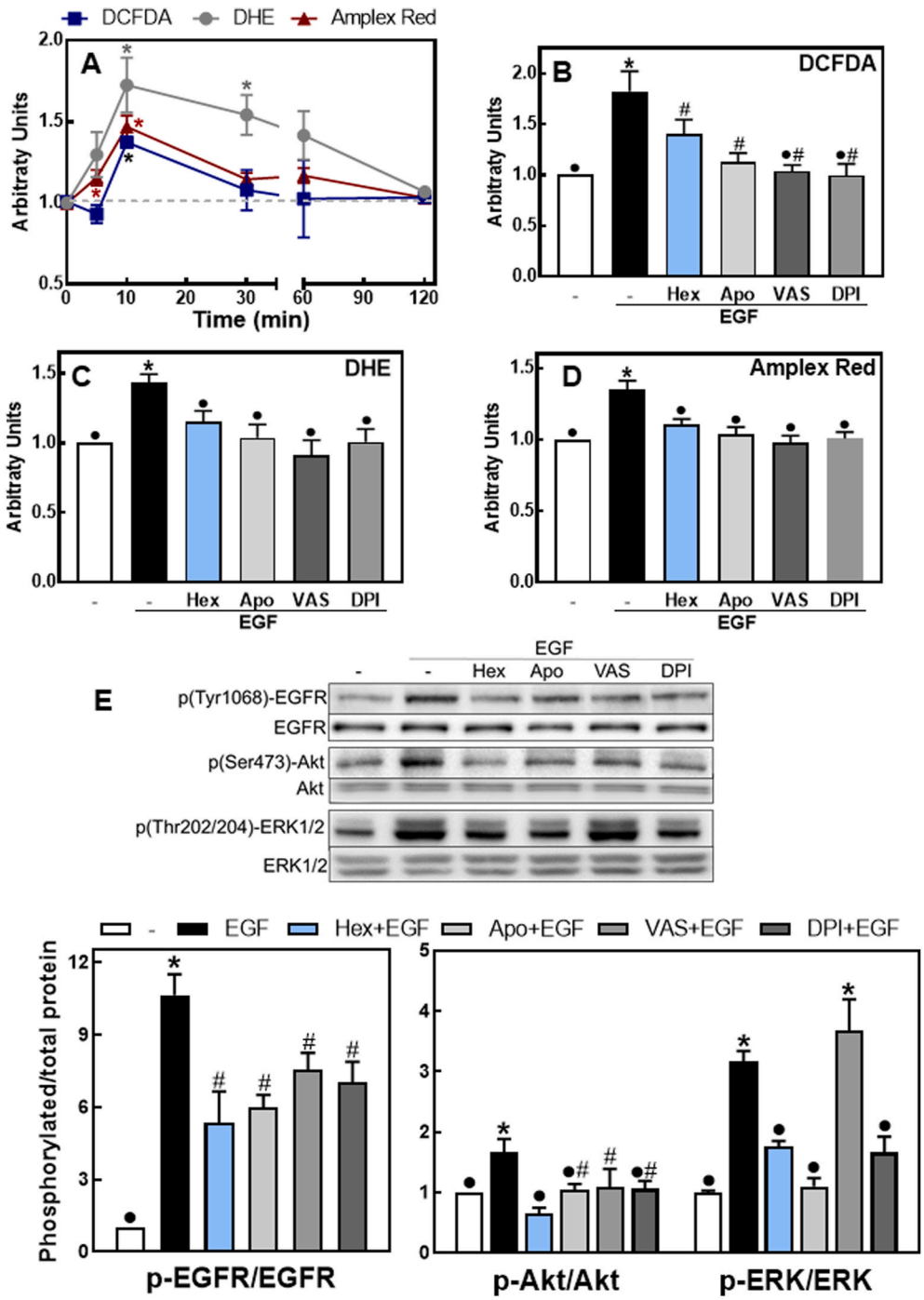

Fig. 5. Hex and NOX inhibitors mitigate EGF-mediated increase in ROS production and EGFR signaling activation. A- Kinetics (0–2 h) of EGF-triggered oxidant production evaluated using the probes DCFDA (blue squares), DHE (grey circles) and Amplex red (red triangles), as described in methods. *Significantly different from cells incubated in the absence of additions (dashed line). (**B-E**) Caco-2 cells were pre-incubated without or with 5 μM Hex (Hex), 1 μM apocynin (Apo), 1 μM VAS-2870 (VAS) or 1 μM DPI (DPI) for 30 min at 37 °C and subsequently incubated in the absence/presence of EGF (10 ng/ml) for 10 min at 37 °C. (**B-D**) ROS production was measured with (**B**) DCFDA, (**C**) DHE or (**D**) Amplex red. (**E**) Phosphorylation levels of EGFR p (Tyr1068), ERK1/2 p (Thr202/204) and Akt p (Ser473) were evaluated as described in the legend to Fig. 3. Results are shown as mean ± SEM and are the average of at least four independent experiments. (**B-E**) Values having different superscripts are significantly different ($p < 0.05$, One way ANOVA). (For interpretation of the references to color in this figure legend, the reader is referred to the Web version of this article.)

increases in cellular ROS and associated EGFR activation. ROS were assessed using three different probes; Amplex red, DCFDA and DHE. The fluorescence increase for the three probes reached a maximum after 10 min incubation of Caco-2 cells in the presence of EGF (Fig. 5A). At this time point, Hex and the NOX inhibitors apocynin, VAS-2870 and DPI either partially (DCFDA) or fully (DHE, Amplex red) inhibited EGF-mediated fluorescence increases (Fig. 5 B-D). We next investigated the effects of apocynin, VAS-2870 and DPI on EGFR phosphorylation in Tyr1068 and downstream phosphorylation of ERK1/2 (Thr202/Tyr204) and Akt (Ser 473) (Fig. 5E). Similarly to that observed for 5 μM Hex, after 10 min incubation with EGF, NOX inhibitors caused a partial inhibition of EGFR Tyr1068 phosphorylation and a total or partial inhibition of ERK1/2 and Akt phosphorylation. The only exception was a lack of VAS-2870 effect on EGF-triggered ERK1/2 phosphorylation.

3.6. *Hex affected EGFR activation and localization at plasma membrane lipid rafts*

The EGFR localizes within lipid rafts [40] and previous studies demonstrated that Hex could interact with the plasma membrane at the level of raft domains [28]. Therefore, we first determined the effects of Hex on the EGFR distribution within the plasma membrane of Caco-2 cells. Plasma membrane lipid rafts were isolated on a density gradient using a detergent-free method. Six fractions were collected and analyzed by Western Blot for flotillin-1, EGFR and p (Tyr 1068)-EGFR levels. Flotillin-1, a protein localized at lipid rafts, was used as marker of lipid

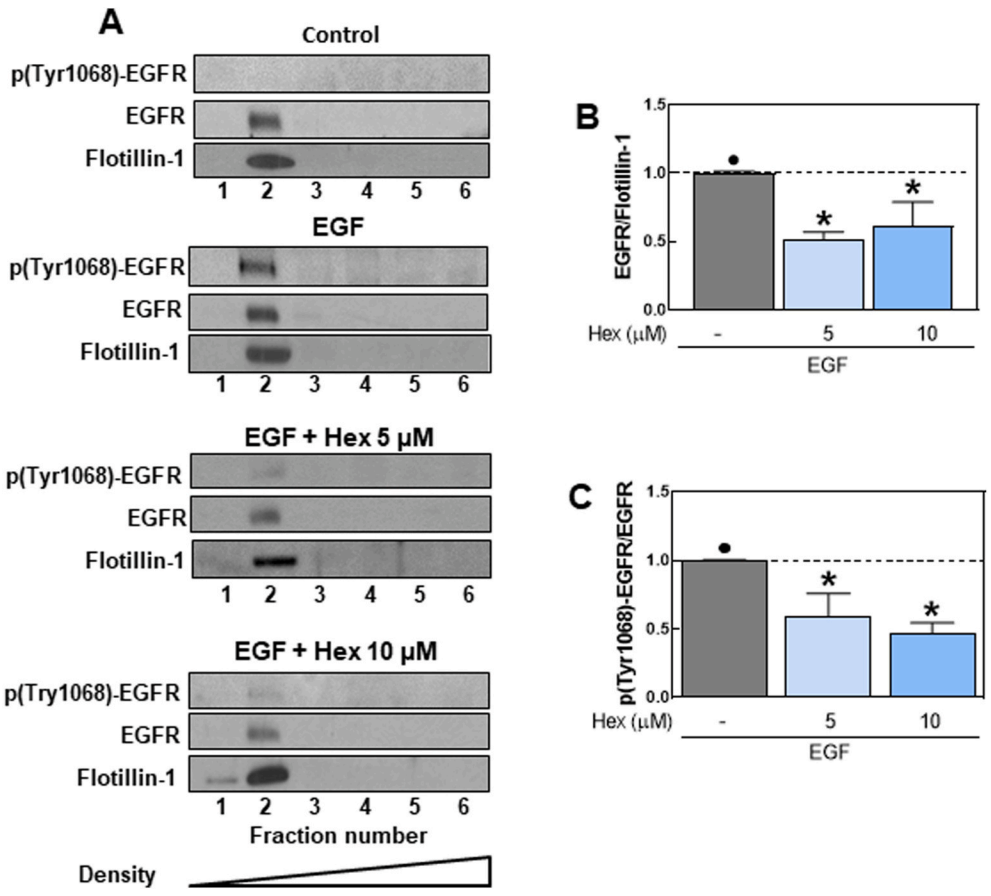

Fig. 6. Effects of Hex on EGFR distribution and Tyr 1068 phosphorylation in lipid rafts.
Detergent-free lipid rafts were isolated from Caco-2 cells treated with/without Hex (5, 10 μM) for 30 min at 37 °C and incubated in the absence/presence of EGF (10 ng/ml) for 10 min at 37 °C. Gradients were separated into 6 fractions and each fraction was analyzed by SDS-PAGE and immunoblotted with the indicated antibodies. (**A**) Representative images for EGFR localization and phosphorylation at lipid rafts. After quantification of bands in fraction 2 (lipid rafts fraction) EGFR (**B**) and p-(Tyr1068)-EGFR (**C**) levels were referred to flotillin-1 and total EGFR content, respectively. (**B**) Results were referred to control values (1, dashed line). Results are shown as means ± SEM of four independent experiments. Values having different superscripts are significantly different ($p < 0.05$, One way ANOVA).

rafts-containing fractions. EGFR and flotillin-1 both localized in fraction 2, confirming the presence of the receptor within lipid raft microdomains of the Caco-2 cell plasma membrane (Fig. 6A). We next investigated if Hex could alter EGFR localization at lipid rafts, as such effect could inhibit EGF-induced EGFR activation/dimerization. Results showed that 5 and 10 μM Hex decreased (40–50%) the localization of the EGFR at lipid rafts and inhibited EGF-induced Tyr 1068 phosphorylation of raft-located EGFR (Fig. 6B and C).

3.7. Hex increased EGFR internalization

Recent studies suggested the importance of lipid rafts in mediating EGFR endocytosis [41]. Thus, we next examined the effects of Hex on EGFR internalization using a cell-ELISA assay. Fig. 7A shows cell surface EGFR levels in Caco-2 cells treated with 2.5, 5 and 10 μM Hex for 30 min at 37 °C in the presence of 10 ng/ml EGF. The percentage of EGFR present at the cell membrane decreased in a dose-dependent manner in cells incubated with Hex and EGF compared to cells treated only with EGF. In the presence of EGF, Hex caused a 30% and 36% decrease in EGFR localized at the cell membrane at 5 and 10 μM concentrations, respectively. Moreover, the internalization occurred even when Hex was removed from the medium after 30 min of pre-incubation, and before EGF addition (Fig. 7A). Hex also promoted EGFR internalization in the absence of EGF stimulation (Fig. 7B). After 30 min incubation, Hex caused a significant reduction (22%) of cell membrane EGFR only at 10 μM concentration. Similar effects were observed without or with removal of Hex from the medium after the 30 min pre-incubation (Fig. 7B). The above results support Hex-mediated internalization of the EGFR receptor.

3.8. Hex promoted EGFR redistribution from the cell membrane to the cytoplasm

The potential effects of Hex on EGFR subcellular localization were evaluated by confocal microscopy. In serum-starved conditions, EGFR (green fluorescence) was located along the plasma membrane (Fig. 8). In Hex-treated cells, at time 0 which corresponds to 30 min preincubation with Hex pretreatment, EGFR showed a diffuse localization throughout the cytoplasm. These findings are consistent with results on EGFR internalization evaluated by cell-ELISA assay (Fig. 7). In EGF-stimulated Caco-2 cells, both in the absence and the presence of Hex, the diffuse cytoplasmic EGFR-fluorescence was consistent with EGFR internalization. After 20 min incubation, EGFR fluorescence co-localized with the red fluorescence of LAMP-1, a lysosomal marker. These results suggest that Hex can promote EGFR internalization and drive its lysosomal degradation.

3.9. Hex-induced EGFR tyr 1045 phosphorylation promotes c-Cbl-mediated ubiquitination

Following internalization, the EGFR can be either recycled back to the plasma membrane or sorted to lysosomes for degradation. EGFR endocytosis stimulated by ubiquitination leads the receptor to lysosomal degradation terminating the signaling cascade [42]. The Cbl ubiquitin ligases, especially c-Cbl, were found to be responsible for EGFR ubiquitination through their direct interaction with EGFR *p*-Tyr 1045 residues [43]. We next assessed whether Hex-mediated EGFR internalization was associated with an increased receptor ubiquitination. Results showed that in EGF-stimulated cells, 5 μM Hex caused 40% higher EGFR Tyr 1045 phosphorylation levels compared to the effect of EGF alone (Fig. 9A). Since phosphorylation at Tyr 1045 creates docking

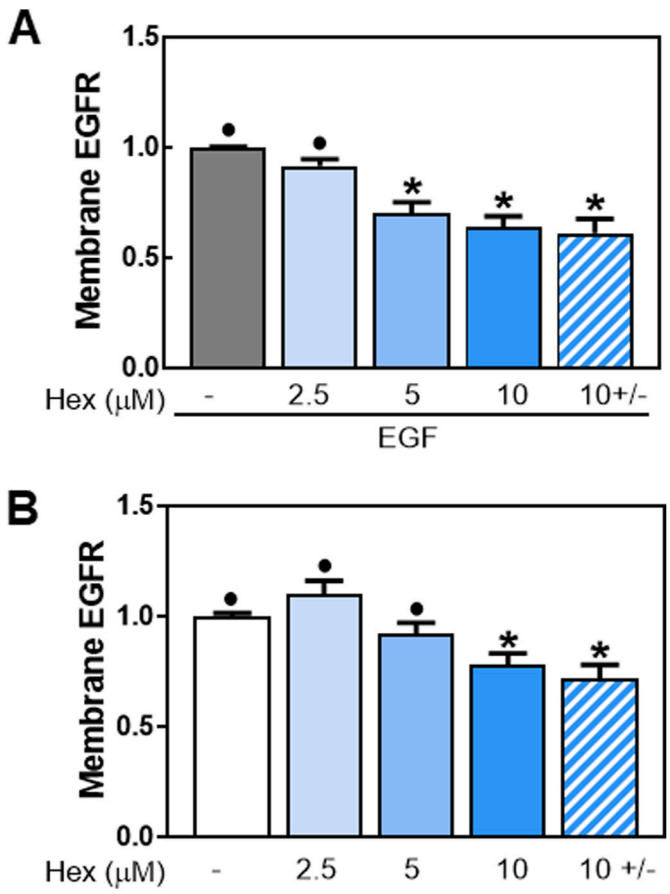

Fig. 7. Effects of Hex on EGFR internalization. Caco-2 cells were treated with 2.5, 5, and 10 μM Hex for 30 min at 37 °C in the presence (**A**) or the absence (**B**) of 10 ng/ml EGF, then incubated at 4 °C for 30 min to allow ligand-receptor binding, and lastly, cells were placed at 37 °C for 15 min to allow receptor internalization. The Hex 10 ± condition corresponds to cells from which Hex was removed after 30 min of pre-incubation. The amount of cell surface EGFR was measured by cell-ELISA assay with an *anti*-EGFR antibody as described in Methods. Values were referred to those for: (**A**) cells treated only with EGF and (**B**) cells incubated in the absence of EGF. Results are shown as means ± SEM of three independent experiments. Values having different superscripts are significantly different ($p < 0.05$, One way ANOVA).

site for the binding of endogenous ubiquitin ligases, we next assessed by EGFR immunoprecipitation, the binding of c-Cbl and ubiquitin. Western blots showed that Hex promoted c-Cbl binding to the EGFR and EGFR ubiquitination upon EGF-stimulation (Fig. 9B).

4. Discussion

This work showed that Hex could exert anti CRC effects through its capacity to inhibit the EGFR pathway. Hex acted decreasing EGFR location at lipid rafts, attenuating EGF-induced EGFR dimerization, activation and internalization, decreasing NOX-dependent ROS production and inhibiting EGFR downstream activation of pro-proliferative and anti-apoptotic pathways, i.e. Raf/MEK/ERK1/2 and PI3K/Akt. Evidence also supports the capacity of Hex to promote EGFR degradation via the ubiquitin/proteasome pathway. Additionally, Hex and the EGFR-targeted chemotherapeutic drug Erlotinib had synergistic actions decreasing Caco-2 cell growth.

EGFR-targeted therapies have been developed and validated to treat different types of tumors, including CRC. However, increasing number and complexity of resistance mechanisms have limited the efficacy of these drugs [44]. For this reason, the identification of compounds that can target the EGFR through novel therapeutic and dietary strategies is an important goal both in the chemoprevention and treatment of EGFR-dependent tumors. PAC have been proposed to be an important class of bioactive compounds relevant in chemoprevention because of epidemiological evidence [21,45,46] and of their capacity to inhibit tumor cell growth both *in vivo* and *in vitro* [17,27,47,48]. In addition, studies have reported that PAC, used in combination with canonical chemotherapeutic drugs, enhance the efficacy of treatments [49]. Previous work from our laboratory showed that Hex could induce apoptosis and cell cycle G_2/M phase arrest in the human CRC Caco-2 cell line [27]. The present follow-up work shows that large procyanidins in part exert anti-CRC actions through the modulation of the lipid raft-associated receptor EGFR.

Cells expressing high level of EGFR, as the Caco-2 cell line [50], often show anticancer drug resistance [51]. We observed that Erlotinib only partially inhibited Caco-2 cell growth and that the synergistic anti-proliferative effect of the combination was mainly due to the inhibitory action of Hex. Hex and Erlotinib also interacted at decreasing EGFR phosphorylation. The synergism between PAC and Erlotinib also supports the EGFR signaling pathway as a target of Hex anti-CRC actions. In fact, Hex inhibited EGFR activating phosphorylation (Tyr 1068) and downstream canonical activation of ERK1/2 and PI3K/Akt cascades, which are the two major proliferative and anti-apoptotic signaling pathways controlled by the receptor. The over-activation of these pathways is frequently observed in CRC, constituting a relevant target in cancer therapy [52–54]. Overall, the above findings emphasize the importance of PAC both: i) as components of a healthy diet that could contribute to decrease the risk for CRC development, and ii) as a potential component of combination therapies for CRC treatment.

Hex inhibited EGF-triggered EGFR internalization after cell pre-incubation with Hex and subsequent incubation with EGF in the absence and in the presence of Hex. Similarly, even after removal from the cell media, Hex inhibited TNFα-triggered activation of NF-κB [25]. These findings suggest that an interaction of Hex with the ligand (EGF) is not an underlying mechanism in the inhibition of the EGFR signaling pathway. It also agrees with previous findings showing the capacity of Hex to interact with membranes [55]. Within the plasma membrane Hex particularly interacts with lipid rafts [28] We currently observed that Hex decreased the presence of EGFR in these domains. EGFR localization at lipid rafts regulates the ability of the receptor to dimerize and *trans*-phosphorylate [56]. Thus, Hex could inhibit the activation of the EGFR, i.e. dimerization upon ligand binding and activation (Tyr1068 phosphorylation), through a direct interaction with the receptor and/or by changing the EGFR membrane environment through Hex binding to lipid rafts.

Redox-regulated mechanisms contribute to enhance and prolong EGFR activation [31]. A transient elevation of cellular ROS due to NOX activation occurs upon binding of EGF to the EGFR [39]. This causes the oxidation of a critical cysteine residue within protein tyrosine phosphatases (PTPs) leading to enzyme inactivation. PTPs inactivate the EGFR via the removal of key EGFR phospho tyrosine groups. Other redox-regulated mechanism of EGFR inactivation involves the oxidation of a Cys797 residue within the receptor that occurs upon EGF binding and recruitment of NOX2 [57]. This oxidation increases the receptor tyrosine kinase activity [57]. Both, PTPs inactivation and EGFR tyrosine kinase activation can enhance and prolong the EGFR-regulated pathway. In agreement with previous findings of EGF-triggered NOX activation, we observed that EGF-mediated ROS transient increase was prevented by Hex and three NOX inhibitors. All these compounds also partially prevented EGFR Tyr 1068 phosphorylation, and caused full or partial inhibition of downstream Akt and ERK activation. The observed lack of effect of Vas-2870 on ERK1/2 phosphorylation could be due to Vas-2870 effects that are independent of EGFR-mediated ERK1/2 activation. Overall, results support the concept that the inhibition of NOX and consequent decreased $O_2^{\cdot-}/H_2O_2$ production in part contribute to the inhibition by Hex of EGF-mediated EGFR activation. Recent evidence showed that dysregulation of cell redox balance also affects EGFR

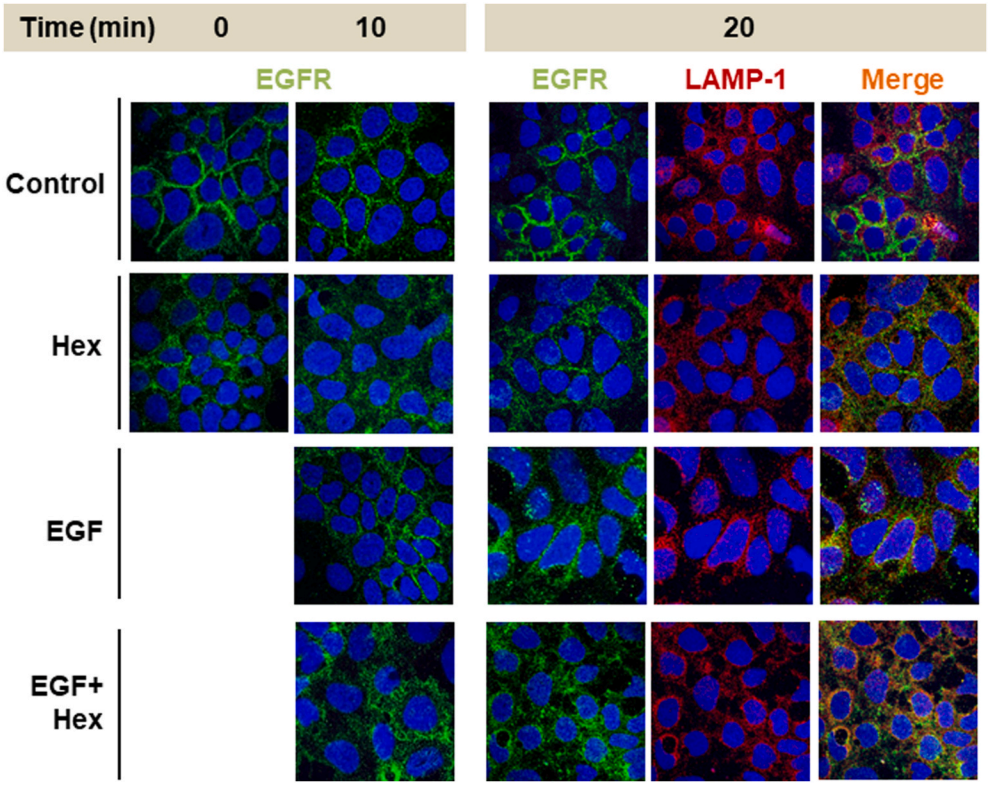

Fig. 8. Effect of Hex on the internalization and localization of the EGFR. Caco-2 cells were incubated with 10 μM Hex for 30 min at 37 °C and subsequently in the absence/presence of EGF (10 ng/ml) for 10 and 20 min. Cells were fixed, permeabilized, and incubated with antibodies for EGFR (green fluorescence) and LAMP1 (red fluorescence). Nuclei were stained using Hoescht 33,342 (blue fluorescence). Confocal images were acquired. Yellow fluorescence indicates co-localization of EGFR and LAMP-1. . (For interpretation of the references to color in this figure legend, the reader is referred to the Web version of this article.)

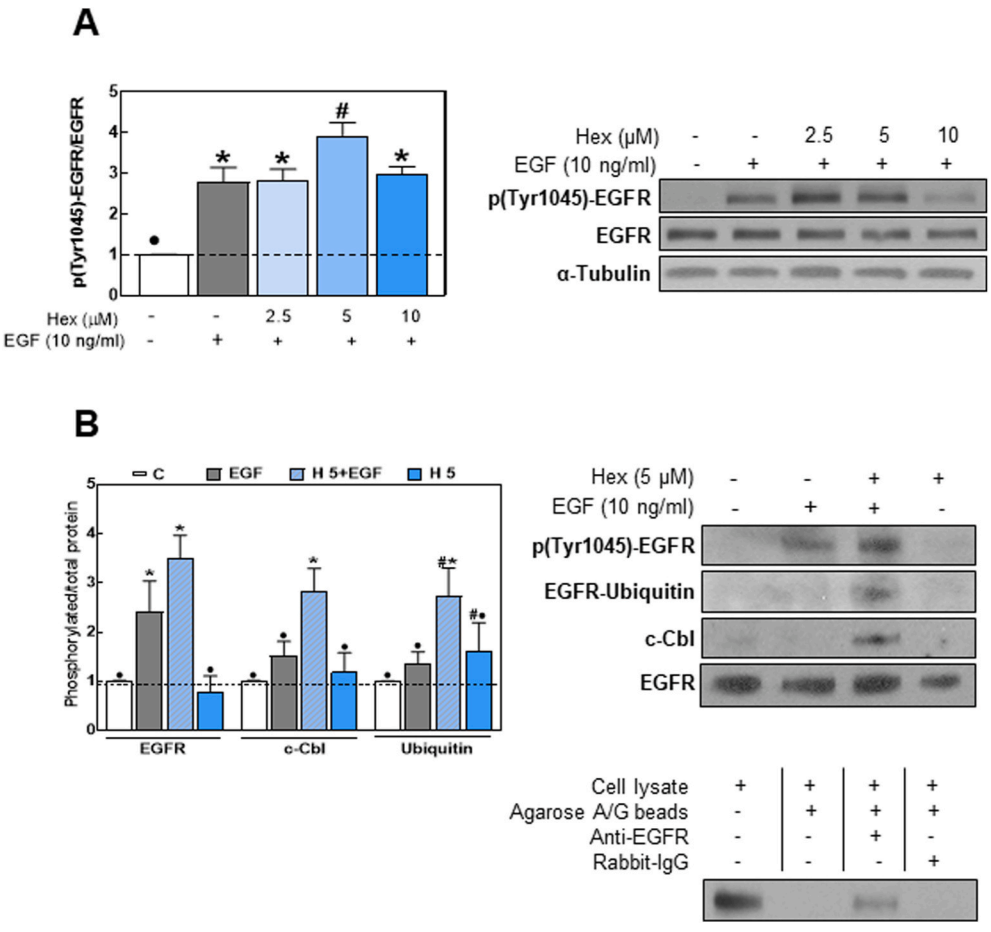

Fig. 9. Hex upregulates events leading to EGFR internalization and degradation. (**A**) Serum starved Caco-2 cells were incubated with/without Hex (2.5, 5, 10 μM) for 30 min and subsequently in the absence/presence of EGF (10 ng/ml) for 10 min. EGFR phosphorylation at Tyr 1045 was measured by Western blot. (**B, upper panel**) cells were incubated with/without 5 μM Hex for 30 min at 37 °C and subsequently in the absence or presence of 10 ng/ml EGF for 15 min. The EGFR was immunoprecipitated as described in Methods. Levels of p (Tyr1045)-EGFR, ubiquitin, c-Cbl and EGFR were measured in the immunoprecipitate by Western blot. Results are expressed as phosphorylated or co-immunoprecipitated protein/total EGFR levels and were referred to controls (1, dashed line). Results are shown as mean ± SEM of three independent experiments. Values having different superscripts are significantly different ($p < 0.05$, One way ANOVA). (**B, lower panel**): controls for the specificity of the immunoprecipitation. Images of whole membranes for each protein are included in Supplemental Fig. 1.

nuclear localization and EGF-regulated gene expression in lung tumor cells, promoting tumorigenesis [58]. Although we have not measured these nuclear events, the redox regulation of EGFR nuclear localization could be another potential mechanism involved in the modulation by Hex of the EGFR pathway.

Hex promoted EGFR internalization both in the absence and in the presence of EGF. Internalized EGFR can eventually continue signaling from endosomes, and subsequently be degraded into lysosome or recycled to the plasma membrane [59]. The phosphorylation of the EGFR at Tyr1045 provides a docking site for the ubiquitin ligase c-Cbl, resulting in EGFR ubiquitylation. This signals the removal of the receptor from the cell membrane via endocytosis into an early endosomal compartment for subsequent degradation [60,61]. In support of the involvement of this mechanism in the action of Hex on EGFR internalization, in EGF-stimulated Caco-2 cells, Hex promoted EGFR Tyr 1045 phosphorylation, the binding of c-Cbl and receptor ubiquitylation. Given that the EGFR could continue to signal from endosomes after its internalization [62], receptor lysosomal degradation and termination of the cascade is a crucial event in inhibiting this oncogenic pathway. In support of such mechanism, immunohistochemistry analysis showed that Hex promoted EGFR internalization and targeted the receptor to lysosomes. Cholesterol- and sphingolipid-enriched raft domains shape the localization of EGFR at the plasma membrane, and determine the ability of the receptor to internalize [63]. Disruption of cholesterol-containing domains induces EGFR clustering and inhibits endocytosis [64,65]. Findings that Hex preferentially binds cholesterol at both Caco-2 cell membranes and lipid-like liposomes [28] suggest that these interactions can participate in the currently observed capacity of Hex to promote EGFR internalization.

In Caco-2 cells, the EGF receptor was found associated with flotillin-1 within raft domains and it has been demonstrated that in mammal cells, endocytosis of flotillin-1-containing cargos is clathrin-independent (NCE) [66]. Physiologically, the EGFR-NCE pathway occurs at high EGF concentrations (>10–100 ng/ml), requires EGFR ubiquitylation, and is critical for the negative regulation of EGFR signaling by directing the receptor to lysosomes for degradation [67,68]. Current evidence suggest that Hex induced EGFR endocytosis through the flotillin-1-associated NCE route which defines receptor fate towards ubiquitination and degradation in EGF-stimulated cells. In the absence of Hex and at a high, nearly saturating, concentration of EGF (10 ng/ml), EGFR phosphorylation at Tyr 1045 increased, but c-Cbl binding and ubiquitylation did not follow up. This suggests that this mechanism of negative regulation of EGFR signaling is impaired in Caco-2 cells even in the presence of excess stimulus. Such alteration would contribute to the overactivation of the EGFR pathway and the promotion of cell proliferation and resistance to apoptosis. Importantly, Hex reactivated EGFR Tyr1045 phosphorylation, c-Cbl binding and EGFR ubiquitylation which would promote EGFR degradation and contribute to signaling inactivation and cell growth inhibition.

In summary, the present study provides evidence that the capacity of high molecular weight PAC to exert anti-proliferative and pro-apoptotic actions in CRC cells occurs in part through the inhibition of EGFR-initiated signaling cascades. Hex acted modulating the EGFR pathway at different levels and through redox and non-redox mechanisms including: i) the inhibition of EGFR dimerization, ii) the inhibition of EGF-mediated activation of NOX and $O_2^{\cdot-}/H_2O_2$ production, decreasing EGFR activation/duration, iii) the promotion of EGFR internalization, and iv) the upregulation of EGFR degradation pathways. Considering that the over-activation or over-expression of the EGFR is implicated in the carcinogenic transformation of normal intestinal epithelial cells, the identification of dietary compounds that inactivate the EGFR, would help design dietary strategies for cancer chemoprevention. Furthermore, the synergistic activity of Hex with Erlotinib stresses the relevance of diet-chemotherapy interactions in optimizing anti CRC therapeutic approaches.

Declaration of competing interest

Authors have no conflict of interest to declare.

Acknowledgements

This work was supported by grants from NIFA-USDA (CA-D*-NUTR-7244-H) and the Packer-Wentz Endowment to P.O., and grants from Universidad de Buenos Aires (20020160100050BA) and CONICET (PIP 0567), Argentina, to A.A. Part of this study was conducted when E. Daveri was a Fellow of MIUR (Doctoral Courses, 28th cycle). W.Z. is the recipient of a fellowship from the Postdoctoral International Exchange Program, China Postdoctoral Council.

Appendix A. Supplementary data

Supplementary data to this article can be found online at https://doi.org/10.1016/j.redox.2020.101830.

Author contributions

P·I.O. and E.D. designed the research. E.D., A.M.A., E.A. and W.Z. performed the experiments. All authors participated in the analysis and discussion of data. E.D. and P·I.O. wrote the paper with editing from all authors.

References

[1] J. Schlessinger, Receptor tyrosine kinases: legacy of the first two decades, Cold Spring Harb Perspect Biol 6 (3) (2014).
[2] M.A. Lemmon, J. Schlessinger, Cell signaling by receptor tyrosine kinases, Cell 141 (7) (2010) 1117–1134.
[3] B. Pabla, M. Bissonnette, V.J. Konda, Colon cancer and the epidermal growth factor receptor: current treatment paradigms, the importance of diet, and the role of chemoprevention, World J. Clin. Oncol. 6 (5) (2015) 133–141.
[4] S. Sigismund, D. Avanzato, L. Lanzetti, Emerging functions of the EGFR in cancer, Mol Oncol 12 (1) (2018) 3–20.
[5] P. Seshacharyulu, M.P. Ponnusamy, D. Haridas, M. Jain, A.K. Ganti, S.K. Batra, Targeting the EGFR signaling pathway in cancer therapy, Expert Opin. Ther. Targets 16 (1) (2012) 15–31.
[6] F. Bray, J. Ferlay, I. Soerjomataram, R.L. Siegel, L.A. Torre, A. Jemal, Global cancer statistics 2018: GLOBOCAN estimates of incidence and mortality worldwide for 36 cancers in 185 countries, Ca - Cancer J. Clin. 68 (6) (2018) 394–424.
[7] R.B. Cohen, Epidermal growth factor receptor as a therapeutic target in colorectal cancer, Clin. Colorectal Canc. 2 (4) (2003) 246–251.
[8] L. Vecchione, B. Jacobs, N. Normanno, F. Ciardiello, S. Tejpar, EGFR-targeted therapy, Exp. Cell Res. 317 (19) (2011) 2765–2771.
[9] F. Di Nicolantonio, M. Martini, F. Molinari, A. Sartore-Bianchi, S. Arena, P. Saletti, S. De Dosso, L. Mazzucchelli, M. Frattini, S. Siena, A. Bardelli, Wild-type BRAF is required for response to panitumumab or cetuximab in metastatic colorectal cancer, J. Clin. Oncol. 26 (35) (2008) 5705–5712.
[10] J. Gong, M. Cho, M. Fakih, RAS and BRAF in metastatic colorectal cancer management, J. Gastrointest. Oncol. 7 (5) (2016) 687–704.
[11] A.J. Weickhardt, T.J. Price, G. Chong, V. Gebski, N. Pavlakis, T.G. Johns, A. Azad, E. Skrinos, K. Fluck, A. Dobrovic, R. Salemi, A.M. Scott, J.M. Mariadason, N. C. Tebbutt, Dual targeting of the epidermal growth factor receptor using the combination of cetuximab and erlotinib: preclinical evaluation and results of the phase II DUX study in chemotherapy-refractory, advanced colorectal cancer, J. Clin. Oncol. 30 (13) (2012) 1505–1512.
[12] I. Palumbo, S. Piattoni, V. Valentini, V. Marini, P. Contavalli, M. Calzuola, F. M. Vecchio, D. Cecchini, F. Falzetti, C. Aristei, Gefitinib enhances the effects of combined radiotherapy and 5-fluorouracil in a colorectal cancer cell line, Int. J. Colorectal Dis. 29 (1) (2014) 31–41.
[13] A.R. Amin, O. Kucuk, F.R. Khuri, D.M. Shin, Perspectives for cancer prevention with natural compounds, J. Clin. Oncol. 27 (16) (2009) 2712–2725.
[14] Y.H. Li, Y.B. Niu, Y. Sun, F. Zhang, C.X. Liu, L. Fan, Q.B. Mei, Role of phytochemicals in colorectal cancer prevention, World J. Gastroenterol. 21 (31) (2015) 9262–9272.
[15] L. Ricciardiello, F. Bazzoli, V. Fogliano, Phytochemicals and colorectal cancer prevention–myth or reality? Nat. Rev. Gastroenterol. Hepatol. 8 (10) (2011) 592–596.
[16] C.G. Fraga, P.I. Oteiza, Dietary flavonoids: role of (-)-epicatechin and related procyanidins in cell signaling, Free Radic. Biol. Med. 51 (4) (2011) 813–823.
[17] F. Gossé, S. Guyot, S. Roussi, A. Lobstein, B. Fischer, N. Seiler, F. Raul, Chemopreventive properties of apple procyanidins on human colon cancer-derived metastatic SW620 cells and in a rat model of colon carcinogenesis, Carcinogenesis 26 (7) (2005) 1291–1295.

[18] R. Zhang, Q. Yu, W. Lu, J. Shen, D. Zhou, Y. Wang, S. Gao, Z. Wang, Grape seed procyanidin B2 promotes the autophagy and apoptosis in colorectal cancer cells via regulating PI3K/Akt signaling pathway, OncoTargets Ther. 12 (2019) 4109–4118.
[19] X. He, L.M. Sun, Dietary intake of flavonoid subclasses and risk of colorectal cancer: evidence from population studies, Oncotarget 7 (18) (2016) 26617–26627.
[20] M. Rossi, C. Bosetti, E. Negri, P. Lagiou, C. La Vecchia, Flavonoids, proanthocyanidins, and cancer risk: a network of case-control studies from Italy, Nutr. Canc. 62 (7) (2010) 871–877.
[21] M. Rossi, E. Negri, M. Parpinel, P. Lagiou, C. Bosetti, R. Talamini, M. Montella, A. Giacosa, S. Franceschi, C. La Vecchia, Proanthocyanidins and the risk of colorectal cancer in Italy, Cancer Causes Control 21 (2) (2010) 243–250.
[22] Y.Y. Choy, G.K. Jaggers, P.I. Oteiza, A.L. Waterhouse, Bioavailability of intact proanthocyanidins in the rat colon after ingestion of grape seed extract, J. Agric. Food Chem. 61 (1) (2013) 121–127.
[23] M. Da Silva, G.K. Jaggers, S.V. Verstraeten, A.G. Erlejman, C.G. Fraga, P.I. Oteiza, Large procyanidins prevent bile-acid-induced oxidant production and membrane-initiated ERK1/2, p38, and Akt activation in Caco-2 cells, Free Radic. Biol. Med. 52 (1) (2012) 151–159.
[24] A.G. Erlejman, C.G. Fraga, P.I. Oteiza, Procyanidins protect Caco-2 cells from bile acid- and oxidant-induced damage, Free Radic. Biol. Med. 41 (8) (2006) 1247–1256.
[25] A.G. Erlejman, G. Jaggers, C.G. Fraga, P.I. Oteiza, TNFalpha-induced NF-kappaB activation and cell oxidant production are modulated by hexameric procyanidins in Caco-2 cells, Arch. Biochem. Biophys. 476 (2) (2008) 186–195.
[26] Y. Xia, S. Shen, I.M. Verma, NF-kappaB, an active player in human cancers, Cancer Immunol Res 2 (9) (2014) 823–830.
[27] Y.Y. Choy, M. Fraga, G.G. Mackenzie, A.L. Waterhouse, E. Cremonini, P.I. Oteiza, The PI3K/Akt pathway is involved in procyanidin-mediated suppression of human colorectal cancer cell growth, Mol. Carcinog. 55 (12) (2016) 2196–2209.
[28] S.V. Verstraeten, G.K. Jaggers, C.G. Fraga, P.I. Oteiza, Procyanidins can interact with Caco-2 cell membrane lipid rafts: involvement of cholesterol, Biochim. Biophys. Acta 1828 (11) (2013) 2646–2653.
[29] M.E. Irwin, K.L. Mueller, N. Bohin, Y. Ge, J.L. Boerner, Lipid raft localization of EGFR alters the response of cancer cells to the EGFR tyrosine kinase inhibitor gefitinib, J. Cell. Physiol. 226 (9) (2011) 2316–2328.
[30] F. Mollinedo, C. Gajate, Lipid rafts as major platforms for signaling regulation in cancer, Adv Biol Regul 57 (2015) 130–146.
[31] D.E. Heppner, A. van der Vliet, Redox-dependent regulation of epidermal growth factor receptor signaling, Redox Biol 8 (2016) 24–27.
[32] I.V. Bijnsdorp, E. Giovannetti, G.J. Peters, Analysis of Drug Interactions, Cancer Cell Culture: Methods and Protocols, second ed., vol. 731, 2011, pp. 421–434.
[33] T.C. Chou, P. Talalay, Quantitative analysis of dose-effect relationships: the combined effects of multiple drugs or enzyme inhibitors, Adv. Enzym. Regul. 22 (1984) 27–55.
[34] M.M. Bradford, A rapid and sensitive method for the quantitation of microgram quantities of protein utilizing the principle of protein-dye binding, Anal. Biochem. 72 (1976) 248–254.
[35] A. Wojtala, M. Bonora, D. Malinska, P. Pinton, J. Duszynski, M.R. Wieckowski, Methods to monitor ROS production by fluorescence microscopy and fluorometry, Methods Enzymol. 542 (2014) 243–262.
[36] H.F. Turk, R.S. Chapkin, Analysis of epidermal growth factor receptor dimerization by BS(3) cross-linking, Methods Mol. Biol. 1233 (2015) 25–34.
[37] J.L. Macdonald, L.J. Pike, A simplified method for the preparation of detergent-free lipid rafts, J. Lipid Res. 46 (5) (2005) 1061–1067.
[38] R. Zandi, A.B. Larsen, P. Andersen, M.T. Stockhausen, H.S. Poulsen, Mechanisms for oncogenic activation of the epidermal growth factor receptor, Cell. Signal. 19 (10) (2007) 2013–2023.
[39] S.R. Lee, K.S. Kwon, S.R. Kim, S.G. Rhee, Reversible inactivation of protein-tyrosine phosphatase 1B in A431 cells stimulated with epidermal growth factor, J. Biol. Chem. 273 (25) (1998) 15366–15372.
[40] A. Hryniewicz-Jankowska, K. Augoff, A. Biernatowska, J. Podkalicka, A.F. Sikorski, Membrane rafts as a novel target in cancer therapy, Biochim. Biophys. Acta 1845 (2) (2014) 155–165.
[41] C. Puri, D. Tosoni, R. Comai, A. Rabellino, D. Segat, F. Caneva, P. Luzzi, P.P. Di Fiore, C. Tacchetti, Relationships between EGFR signaling-competent and endocytosis-competent membrane microdomains, Mol. Biol. Cell 16 (6) (2005) 2704–2718.
[42] K. Roepstorff, M.V. Grandal, L. Henriksen, S.L. Knudsen, M. Lerdrup, L. Grovdal, B. M. Willumsen, B. van Deurs, Differential effects of EGFR ligands on endocytic sorting of the receptor, Traffic 10 (8) (2009) 1115–1127.
[43] L.M. Grovdal, E. Stang, A. Sorkin, I.H. Madshus, Direct interaction of Cbl with pTyr 1045 of the EGF receptor (EGFR) is required to sort the EGFR to lysosomes for degradation, Exp. Cell Res. 300 (2) (2004) 388–395.
[44] C.R. Chong, P.A. Janne, The quest to overcome resistance to EGFR-targeted therapies in cancer, Nat. Med. 19 (11) (2013) 1389–1400.
[45] E. Theodoratou, J. Kyle, R. Cetnarskyj, S.M. Farrington, A. Tenesa, R. Barnetson, M. Porteous, M. Dunlop, H. Campbell, Dietary flavonoids and the risk of colorectal cancer, Cancer Epidemiol. Biomark. Prev. 16 (4) (2007) 684–693.
[46] P. Terry, E. Giovannucci, K.B. Michels, L. Bergkvist, H. Hansen, L. Holmberg, A. Wolk, Fruit, vegetables, dietary fiber, and risk of colorectal cancer, J. Natl. Cancer Inst. 93 (7) (2001) 525–533.
[47] V. Nandakumar, T. Singh, S.K. Katiyar, Multi-targeted prevention and therapy of cancer by proanthocyanidins, Canc. Lett. 269 (2) (2008) 378–387.
[48] W. Zhu, M.C. Li, F.R. Wang, G.G. Mackenzie, P.I. Oteiza, The inhibitory effect of ECG and EGCG dimeric procyanidins on colorectal cancer cells growth is associated with their actions at lipid rafts and the inhibition of the epidermal growth factor receptor signaling, Biochem. Pharmacol. 175 (2020) 113923.
[49] K.Y. Cheah, G.S. Howarth, K.A. Bindon, J.A. Kennedy, S.E. Bastian, Low molecular weight procyanidins from grape seeds enhance the impact of 5-Fluorouracil chemotherapy on Caco-2 human colon cancer cells, PloS One 9 (6) (2014), e98921.
[50] S. Skvortsov, B. Sarg, J. Loeffler-Ragg, I. Skvortsova, H. Lindner, H. Werner Ott, P. Lukas, K. Illmensee, H. Zwierzina, Different proteome pattern of epidermal growth factor receptor-positive colorectal cancer cell lines that are responsive and nonresponsive to C225 antibody treatment, Mol. Canc. Therapeut. 3 (12) (2004) 1551–1558.
[51] R. Bianco, T. Troiani, G. Tortora, F. Ciardiello, Intrinsic and acquired resistance to EGFR inhibitors in human cancer therapy, Endocr. Relat. Canc. 12 (Suppl 1) (2005) S159–S171.
[52] J.Y. Fang, B.C. Richardson, The MAPK signalling pathways and colorectal cancer, Lancet Oncol. 6 (5) (2005) 322–327.
[53] J.A. Fresno Vara, E. Casado, J. de Castro, P. Cejas, C. Belda-Iniesta, M. Gonzalez-Baron, PI3K/Akt signalling pathway and cancer, Canc. Treat Rev. 30 (2) (2004) 193–204.
[54] M. Berg, K. Soreide, EGFR and downstream genetic alterations in KRAS/BRAF and PI3K/AKT pathways in colorectal cancer: implications for targeted therapy, Discov. Med. 14 (76) (2012) 207–214.
[55] S.V. Verstraeten, C.L. Keen, H.H. Schmitz, C.G. Fraga, P.I. Oteiza, Flavan-3-ols and procyanidins protect liposomes against lipid oxidation and disruption of the bilayer structure, Free Radic. Biol. Med. 34 (1) (2003) 84–92.
[56] H.F. Turk, R. Barhoumi, R.S. Chapkin, Alteration of EGFR spatiotemporal dynamics suppresses signal transduction, PloS One 7 (6) (2012), e39682.
[57] C.E. Paulsen, T.H. Truong, F.J. Garcia, A. Homann, V. Gupta, S.E. Leonard, K. S. Carroll, Peroxide-dependent sulfenylation of the EGFR catalytic site enhances kinase activity, Nat. Chem. Biol. 8 (1) (2011) 57–64.
[58] A.C. Little, M. Hristova, L. van Lith, C. Schiffers, C.M. Dustin, A. Habibovic, K. Danyal, D.E. Heppner, M.J. Lin, J. van der Velden, Y.M. Janssen-Heininger, A. van der Vliet, Dysregulated redox regulation contributes to nuclear EGFR localization and pathogenicity in lung cancer, Sci. Rep. 9 (1) (2019) 4844.
[59] H.S. Wiley, Trafficking of the ErbB receptors and its influence on signaling, Exp. Cell Res. 284 (1) (2003) 78–88.
[60] T. Ravid, J.M. Heidinger, P. Gee, E.M. Khan, T. Goldkorn, c-Cbl-mediated ubiquitinylation is required for epidermal growth factor receptor exit from the early endosomes, J. Biol. Chem. 279 (35) (2004) 37153–37162.
[61] K. Haglund, S. Sigismund, S. Polo, I. Szymkiewicz, P.P. Di Fiore, I. Dikic, Multiple monoubiquitination of RTKs is sufficient for their endocytosis and degradation, Nat. Cell Biol. 5 (5) (2003) 461–466.
[62] M. Miaczynska, L. Pelkmans, M. Zerial, Not just a sink: endosomes in control of signal transduction, Curr. Opin. Cell Biol. 16 (4) (2004) 400–406.
[63] M. Gueguinou, A. Gambade, R. Felix, A. Chantome, Y. Fourbon, P. Bougnoux, G. Weber, M. Potier-Cartereau, C. Vandier, Lipid rafts, KCa/ClCa/Ca2+ channel complexes and EGFR signaling: novel targets to reduce tumor development by lipids? Biochim. Biophys. Acta 1848 (10 Pt B) (2015) 2603–2620.
[64] N. Bag, S. Huang, T. Wohland, Plasma membrane organization of epidermal growth factor receptor in resting and ligand-bound states, Biophys. J. 109 (9) (2015) 1925–1936.
[65] S. Saffarian, Y. Li, E.L. Elson, L.J. Pike, Oligomerization of the EGF receptor investigated by live cell fluorescence intensity distribution analysis, Biophys. J. 93 (3) (2007) 1021–1031.
[66] O.O. Glebov, N.A. Bright, B.J. Nichols, Flotillin-1 defines a clathrin-independent endocytic pathway in mammalian cells, Nat. Cell Biol. 8 (1) (2006) 46–54.
[67] E. Barbieri, P.P. Di Fiore, S. Sigismund, Endocytic control of signaling at the plasma membrane, Curr. Opin. Cell Biol. 39 (2016) 21–27.
[68] G. Caldieri, E. Barbieri, G. Nappo, A. Raimondi, M. Bonora, A. Conte, L. Verhoef, S. Confalonieri, M.G. Malabarba, F. Bianchi, A. Cuomo, T. Bonaldi, E. Martini, D. Mazza, P. Pinton, C. Tacchetti, S. Polo, P.P. Di Fiore, S. Sigismund, Reticulon 3-dependent ER-PM contact sites control EGFR nonclathrin endocytosis, Science 356 (6338) (2017) 617–624.